

---

## RAMAN GAIN OF MONOCHROMATIC LIGHT IN SINGLE-MODE SILICA FIBERS AND THE FEATURES OF ITS EMERGENCE

P.A. KOROTKOV, G.S. FELINSKYI<sup>1</sup>

UDC 535.375.54  
©2007

Taras Shevchenko Kyiv National University  
(6, Academician Glushkov Ave., Kyiv 03127, Ukraine; e-mail: pak@mail.univ.kiev.ua),  
<sup>1</sup>“Vector” Scientific and Research Institute  
(10a, Ryleev Str., Kyiv 04073, Ukraine; e-mail: felinsky@ndivektor.kiev.ua)

---

Stimulated Raman scattering (SRS) of light comprises the basis of functioning such photonic devices as optical fiber lasers and optical fiber amplifiers. In contrast to previous experiments, where the Raman threshold was determined phenomenologically, we have analyzed the hyper-Raman emission threshold for single-mode fibers in the framework of the rigorous consideration of the Raman gain in active laser materials. Our analysis showed that the Raman laser threshold for a monochromatic optical signal can be calculated directly from the standard equations for coupled waves, making use of only fundamental parameters of the fiber. The quantitative data for the laser threshold value as a function of the wavelength are given for a few widely used Raman fibers.

---

### 1. Introduction

One of the fundamental types of the molecular scattering of light is Raman scattering (RS). This phenomenon actively reveals itself in the entire optical range of electromagnetic radiation. The effect of SRS in optical fibers is accompanied by a huge amplification of a Stokes wave. Nowadays, the Raman amplification comprises a basis for the creation of quantum generators or amplifiers of optical radiation and is widely used for developing such photonic devices as fiber Raman lasers (FRLs) [1] and fiber Raman amplifiers (FRAs) [2] which substantially extended the capacity of modern fiber-optic information transmission systems.

The creation of highly effective Raman continuous-wave medium-power lasers in single-mode fibers for the near infra-red range has been recognized as one of the most prominent achievements in laser physics in the 1990s [1]. In the combination with dispersive resonators,

such lasers can generate radiation with a virtually arbitrary wavelength ranging from 1.1 to 1.6  $\mu\text{m}$  and a high lasing power up to several watts.

The basic feature of Raman lasers is that their functioning is based on the photon-phonon interaction in a substance, which manifests itself as a nonlinear optical effect – SRS. In this connection, FRLs constitute a new class of laser emission sources. The physics of the Raman laser functioning originates from the nonlinear optics of optical fibers. This distinguishes them from conventional lasers (solid-state, gaseous, semiconductor, chemical, and so on) which are based on the electron-photon interaction resulting in a stimulated emission in the medium with inverted population of electron energy levels.

The optical non-linearity of the SRS process is known to manifest itself, first, in the dependence of the Stokes wave intensity on the intensity of a pumping wave. Second, SRS has a gain threshold for the Stokes wave. For the majority of dielectric media, in particular, for silica, the quantum efficiency of spontaneous RS is of the order of  $10^{-6}$ . However, if the pumping power exceeds a certain threshold value, so that the losses for the Stokes wave propagation become compensated, SRS emerges. The amplitudes of Stokes waves quickly increase at that. Provided the phase synchronism of the interaction between the highly intense pumping field and the phonon system of a material, SRS appears as a result of the parametric and coherent accumulation of weak Stokes waves at a significant length. Due to such an accumulation, the Stokes wave gets a so large

amplification that a considerable portion of the pumping energy (of about 80%) can be transformed into the energy of the SRS mode. This case corresponds to the generation of hyper-Raman emission, and a device, where this process occurs, is sometimes dubbed as a single-pass SRS laser. Unfortunately, the absence of the feedback for the Stokes wave in this elementary setup is a source of numerous shortcomings, which ultimately interferes with its practical implication, so that such a scheme is seldom called “laser”, every time emphasizing that it is single-pass.

Therefore, the overwhelming majority of real Raman lasers includes a pump cavity for ensuring a feedback which provides sufficient conditions for the lasing to be effective, in particular, a necessary degree of output radiation monochromaticity. But the pumping threshold of Raman laser differs from the threshold of monochromatic hyper-Raman emission. The Raman laser threshold becomes somewhat higher, namely, by the magnitude of dissipative losses of the optical power in the constructive elements of the cavity’s optical scheme. The optical scheme is subjected to the optimization in order to minimize – and, in the ideal case, to make vanish – the indicated difference, which is a parameter of laser realization. Therefore, the threshold of monochromatic hyper-Raman emission can be regarded as a theoretical minimum of the pumping power, above which the generation in a single-mode Raman laser with an ideal cavity commences. It should be noticed that the impressive progress has been achieved for modern fiber lasers on the way to minimize losses owing to the monolithic integration of optical scheme elements, which is based on the Bragg grating technology and allows gratings to be recorded immediately in single-mode fibers.

A single-mode optical fiber, which is traditionally fabricated of silica glass, is a necessary component of Raman lasers. Just in a fiber, a usual glass, which reveals almost no nonlinearity, transforms into a highly effective nonlinear medium with a very low Raman threshold. This occurs owing to an extremely high concentration of pumping power in the fiber core, which has a transverse cross-section of no more than about  $50 \mu\text{m}^2$ . Therefore, laser generation virtually arises if the pumping power is some tens of milliwatts or lower, and rather short sections of specialized Raman fibers – not longer than a few hundred meters – are used in Raman lasers. At the same time, the low level of intrinsic losses (of about 0.2 dB/km), when light with a wavelength of about  $1.55 \mu\text{m}$  propagates along fibers, allows one to maintain a high intensity of pumping (above the Raman

threshold) for a distance that considerably exceeds 10 km. Hence, the application of a Raman amplifier provides the compensation of losses for the optical signal propagation, which is distributed along a very large section of the fiber, and increases the distance of signal transmission up to several hundred kilometers. Recently, optical transmission lines have been demonstrated, in which a Terabit capacity for a distance over 1000 km has been achieved due to the cascaded application of Raman amplifiers.

Notwithstanding the obvious convenience of experimental measurements of the Raman threshold value, which has been determined in the first experiments [3], it cannot be always used to determine quantitatively the lasing threshold of a Raman laser or signal gain conditions for fiber-optic Raman amplifiers. The hyper-Raman emission arises from a spontaneous Stokes noise with a frequency bandwidth of about 40 THz, which is at least  $10^3$  times broader than the FRL linewidth or the bandwidth of the signal that is amplified in the FRA. From the optical point of view, the lasing line of the FRL and the real optical signal in the FRA are monochromatic electromagnetic waves belonging to the optical range against the background of a non-uniform continuum of optical Stokes noise. Accordingly, the threshold pumping power for the amplification of such monochromatic signals turns out 1.5–2 orders of magnitude lower than the well-known estimations for the Raman threshold [4].

In this work, the lasing threshold is considered in a general theoretical sense as a transformation of the substance from an ordinary Lambert state, which is characterized by the optical wave attenuation, to a state, which is characterized by amplification of an optical signal, provided the Raman interaction between monochromatic waves in single-mode fibers. Such an approach allows one to derive a threshold condition for monochromatic hyper-Raman emission directly from the standard equations for coupled pumping and Stokes emission waves. The threshold condition determines the pumping power, which converts the fiber into the absolute transparency regime, after which, if the pumping power grows, the fiber core becomes a gain medium for a coherent optical wave. Using the results of simulation of the Raman gain profile [5], the frequency dependences of the hyper-Raman emission threshold have been obtained for some widely used fibers; these dependences allow the amplitude of lasing threshold to be determined quantitatively for any frequency from the Stokes-shift range. At last, we illustrate the application of the results of numerical

calculations of the FRL threshold to the analysis of a particular scheme of a multiwave pumping source for an FRA.

## 2. SRS Generation and a Hyperemission Threshold

The theory describes the SRS-assisted gain of Stokes emission at the propagation of the latter along a fiber making use of a reduced equation for the intensities of interacting waves which looks like

$$\frac{dI_s}{dz} = g_R I_p I_s, \quad (1)$$

where  $g_R$  is the Raman gain coefficient, and  $I_p$  and  $I_s$  are the intensities of the pumping and Stokes waves, respectively.

The Raman gain coefficients with respect to intensity,  $g_R$ , and power,  $\tilde{g}_R$ , are coupled with each other by the relation  $\tilde{g}_R = g_R A_{\text{eff}}$ , where  $A_{\text{eff}}$  is the effective area of the fiber core cross-section. One should note that the gain coefficient with respect to intensity  $g_R$  is a merely material parameter of the fiber core and is measured in units of m/W, while the Raman gain coefficient with respect to power  $\tilde{g}_R$  characterizes the fiber in whole and is measured in units of  $(\text{W} \times \text{km})^{-1}$ . Since both those coefficients are unequivocally coupled with each other through the effective area  $A_{\text{eff}}$  which is constant for every specific fiber, we, in what follows, use a single notation  $g_R$  for both gain factors. It will not cause any misunderstanding, if one pays attention to the dimensions of those quantities.

In the framework of the semiclassical consideration of SRS [6], optical radiation can be described by means of classical electromagnetic waves, whereas the molecular system can be examined as a harmonic oscillator which is subjected to the action of an external force. Such a model establishes a relation between the differential polarizability of the molecular system  $\partial\alpha_{ij}/\partial q_k$  and the complex value of nonlinear susceptibility  $\chi^{(3)}$  which is a standard parameter in nonlinear optics:

$$\chi_{ijkl}^{(3)}(\omega) = \frac{N}{12m\epsilon_0 V} \frac{1}{\omega_v^2 - \omega^2 + i\omega\Gamma} \cdot \sum_n \frac{\partial\alpha_{ij}}{\partial q_n} \left( \frac{\partial\alpha_{kl}}{\partial q_n} \right)^*, \quad (2)$$

where  $\omega_v$  is the undamped resonance phonon frequency,  $\omega$  is the actual phonon frequency,  $\Gamma$  is the damping constant,  $q_k$  are the coordinates of the local displacement induced by the time-dependent electric field,  $m$  is the mass associated with vibrations,  $N$  is the number of

oscillators in the interaction volume  $V$ , and  $\epsilon_0$  is the dielectric permittivity of vacuum.

Since optical fibers are manufactured of silica glass, which is an amorphous material, the tensor of the fourth rank  $\chi^{(3)}$  is isotropic. Therefore, it has only 21 components different from zero; the indices of those components are either equal to each other ( $\chi_{iiii}^{(3)}$ ) or appear in pairs ( $\chi_{ijji}^{(3)}$ ,  $\chi_{ijij}^{(3)}$ , and  $\chi_{ijjj}^{(3)}$ ). Hence, the Raman gain coefficient at the Stokes frequency  $\omega_s = \omega_p - \omega_v$  can be written down in the form [6]

$$g_R(\omega) = -\frac{3\omega_s}{\epsilon_0 c^2 n_p n_s} \frac{\text{Im} \left[ \chi_{iiii}^{(3)}(\omega) + \chi_{ijji}^{(3)}(\omega) \right]}{2A_{\text{eff}}^{ps}}. \quad (3)$$

The susceptibilities of the third order can be considered as such that do not depend on frequency. Then, the gain factor  $g_R$ , besides the linear dependence on the Stokes displacement frequency, also reveals an extra frequency dependence, which is mainly determined by the imaginary part of the nonlinear susceptibility  $\chi^{(3)}$ , i.e. by the resonant denominator in relation (2) for a harmonic phonon oscillator.

In order to calculate the Raman threshold, consider the interaction between Stokes and pumping waves. If pumping is continuous, this interaction is described by the known system of equations which can be written down as follows:

$$\frac{dI_s(z, \omega)}{dz} = g_R(\omega) I_p(z) I_s(\omega, z) - \alpha_s I_s(z, \omega), \quad (4)$$

$$\frac{dI_p(z)}{dz} = \frac{\omega_p}{\omega_s} g_R(\omega) I_p(z) I_s(z, \omega) - \alpha_p I_p(z), \quad (5)$$

where  $\alpha_s$  and  $\alpha_p$  are the absorption coefficients which determine losses at the Stokes and pumping wave frequencies. Actually, Eqs. (4) and (5) describe the variations of the Stokes and pumping wave intensities in a quasicontinuous approximation and if the wave amplitudes vary slowly in the course of wave propagation along the fiber (along the coordinate  $z$ ). The current frequency of interacting waves is included into Eqs. (4) and (5) as a parameter. As concerning the frequency dependence of the quantities that enter into those equations, the following approximations are valid. The pumping line can be considered as infinitely narrow in comparison with a bandwidth of Stokes emission (this means that pumping remains localized at its frequency  $\omega_p$ ). Furthermore,  $I_p(z, \omega) = I_p(z, \omega)|_{\omega=\omega_p} = I_p(z)$  and does not depend on the frequency at any point  $z$  along the fiber. Virtually, Eqs. (4) and (5) describe the Raman interaction between monochromatic pumping and

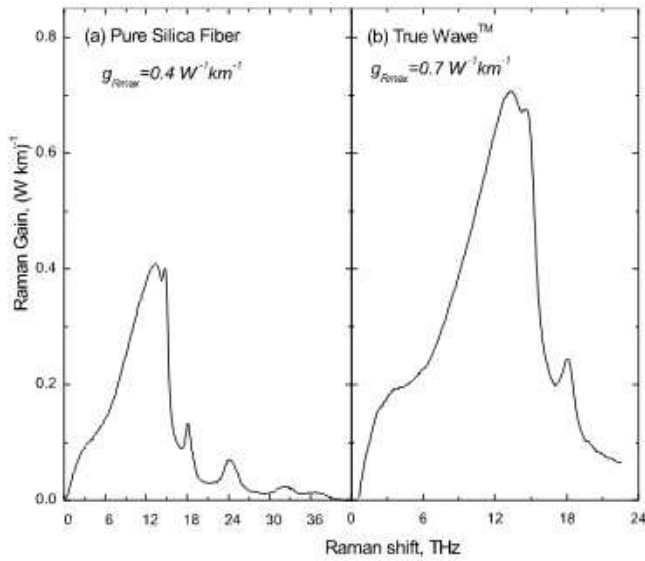


Fig. 1. Raman gain spectra for fused silica-based fibers: (a) a standard silica fiber and (b) a TrueWave RS<sup>TM</sup> fiber

Stokes emission waves. It is natural that the degree of wave coupling at an arbitrary given frequency  $\omega$  of the Stokes wave is unequivocally determined by values of the functions  $g_R(\omega)$  and  $\alpha(\omega)$ . The dependence  $g_R(\omega)$  behaves itself as it is shown in Fig. 1 for the corresponding fiber types, and the dependence  $\alpha(\omega)$ , as a rule, is rather weak. Therefore, the absorption coefficients  $\alpha_s$  and  $\alpha_p$  in Eqs. (4) and (5) can be regarded as constant and independent of the frequency.

In accordance with Eqs. (2) and (3), the Raman gain coefficient  $g_R(\omega)$  is described by the imaginary part of the nonlinear susceptibility  $\chi^{(3)}$  of the third order. In its turn,  $\chi^{(3)}$  is associated with the cross-section of spontaneous RS which is measured experimentally. Every of the numerous active Raman oscillations in the molecular system of a fiber gives its contribution to the formation of the Raman spectrum which has rather complicated shape. Accordingly, the stimulated Raman gain profile manifests itself as a non-uniform continuum. In Fig. 1, the Raman gain curves  $g_R(\omega)$  are depicted for two kinds of optical fibers fabricated on the basis of silica glass which are widely used for optical signal transmission: a fiber of pure fused silica (panel a) and a TrueWave RS<sup>TM</sup> fiber with optimal dispersion (panel b). It is evident that the Raman spectrum depends on the fiber composition and the presence of impurities in its core, so that the maximum of the Raman gain coefficient  $g_{Rmax}$  may vary substantially. An important feature of the Raman spectrum in silica fibers is that the gain curve  $g_R(\omega)$  has a considerable halfwidth (of about 5 THz)

and extends up to frequencies of about 40 THz. This fact results from the non-crystalline structure of silica glass. Owing to this, the Raman gain in silica fibers is continuous in a wide range of frequencies, which allows the optical fibers to be used as an active medium for both broadband amplifiers and FRLs with a wide frequency range of emission line tuning.

The stimulated Raman amplification of an optical wave in a single-mode fiber occurs as follows. If a weak radiation (an information signal) with frequency  $\omega_s$  enters into the fiber together with a pumping wave with frequency  $\omega_p$ , the former will be amplified by the Stokes Raman wave, provided that the frequency difference  $\omega_p - \omega_s$  ranges within the limits of the Raman spectrum bandwidth. The gain ripple, which duplicates the  $g_R(\omega)$  profile, is corrected in practice by making use of several pumping sources, which allow the gain maximum to be set at a required wavelength.

If there is no input optical signal, the pumping radiation excites spontaneous RS at the fiber input and creates a weak signal which acts as a probe wave and becomes more intensive while propagating along the fiber. Since spontaneous RS generates phonons from the Raman spectrum range, all frequency components that fall within this band will be amplified. Certainly, the frequency components located near the maximum of  $g_R(\omega)$  will obtain the maximal gain for the frequency components of the Stokes wave at about  $440\text{ cm}^{-1}$  (about 13.2 THz). Moreover, as soon as the pumping power has exceeded the Raman threshold, these components will be amplified exponentially. Provided an active fiber is placed into a cavity, monochromatic waves at the resonance frequency will obtain the maximal gain. If there is no cavity, SRS may give rise to the generation of the full Stokes continuum, but at much higher powers of pumping.

Certainly, at a rigorous description of SRS, the effect of pumping depletion should be included into consideration, but this phenomenon is usually neglected while estimating the Raman threshold. In this approximation, Eq. (4) has the well-known exact solution

$$I_s(L) = I_s(0) \exp(g_R I_0 L_{\text{eff}} - \alpha_p L), \tag{6}$$

where  $I_0 = I_p(0)$  is the input pumping intensity at  $z = 0$ , and the effective interaction length  $L_{\text{eff}}$  is defined by the expression

$$L_{\text{eff}} = \frac{1}{\alpha_p} [1 - \exp(-\alpha_p L)]. \tag{7}$$

Proceeding from the early experimental works [3, 7, 8], it was common practice to determine the Raman threshold as the input pumping power, at which the power of the Stokes wave becomes equal to the pumping power at the fiber output. Taking into account the obvious convenience of experimental measurement of such a Raman threshold, this quantity is often used (see, e.g., work [4]) for the interpretation of measurement data. There are a few reasons discussed below which make the results of quantitative estimations of this threshold up to 100 times larger than the minimal power of the hyper-Raman emission threshold really measured in experiment.

By definition, the Raman threshold is reached, if the pumping power and the power of gained Stokes emission are equal at the output of a fiber of a certain length. The conditions for the experimental observation of the Raman threshold in a single-mode fiber are schematically illustrated in Fig. 2. The input pumping radiation with power  $P_p$  and a narrow frequency bandwidth, after the Raman interaction in a single-mode fiber (SMF) of length  $L$ , generates the Stokes emission with the peak power equal to the output pumping power:  $P_p(L) = P_s(L)$ .

The required equality of the Stokes emission and pumping powers at the fiber output can be obtained only if the full single-pass gain of the spontaneous Stokes continuum is not lower than 60 dB. This becomes evident if one takes into account that the efficiency of spontaneous RS in silica glass does not exceed  $10^{-6}$ . Such gain magnitude considerably exceeds both the hyper-Raman emission and laser thresholds. Really, in contrast to the threshold concerned, the hyper-Raman emission threshold for an active medium corresponds to such pumping power, at which the amplification of the Stokes wave compensates total losses for its propagation in a fiber.

For the following comparison and in advance of examining the conditions for the Raman laser threshold to appear, we briefly present the known results concerning the estimation of the experimental Raman threshold in a single-mode fiber [4]. In order to determine the power of a Stokes wave, Eq. (6) is usually integrated over the whole frequency interval  $h\omega_s$  of the Raman spectrum, which allows the output power  $P_s(L)$  to be expressed in terms of the effective bandwidth of Stokes emission  $B_{s0}^{\text{eff}}$  around the gain maximum at  $\omega = \omega_s$ . The effective bandwidth of Stokes emission  $B_{s0}^{\text{eff}}$  depends on the pumping intensity  $I_0$ , the second derivative of the gain profile  $g_R''(\omega_s) = (d^2 g_R / d\omega^2)_{\omega=\omega_s}$ , and the fiber length  $L$  and characterizes not only the optical fiber but

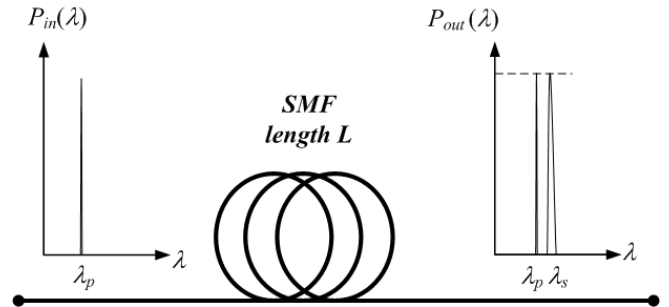


Fig. 2. Experimental setup for the observation of stimulated Raman threshold in a single-mode fiber

also the conditions of RS observation. Afterwards, using the definition of experimental Raman threshold  $P_s(L) = P_p(L) = P_0 \exp(-\alpha_p L)$ , where  $P_0 = I_0 A_{\text{eff}}$  is the input pumping power, and adopting the Lorentzian gain contour, we obtain [4]

$$g_R P_{0p}^{\text{th}} L_{\text{eff}} / A_{\text{eff}} \approx 16, \quad (8)$$

where  $P_{0p}^{\text{th}}$  is the input pumping power which ensures the experimental Raman threshold.

In accordance with the results of work [4], estimation (8) corresponds to forward RS; for backward one, the right-hand side of Eq. (8) equals 20. The relations obtained correspond to the case where the polarizations of the pumping and Stokes waves are identical and kept constant along fibers. Provided that their polarizations change, the Raman threshold increases from 1 to 2. If the polarization is totally destroyed, it reaches the value of 2.

Thus, relation (8) gives a quantitative estimation of the pumping power which ensures the Raman threshold at  $\alpha_p L \gg 1$ , when  $L_{\text{eff}} \approx 1/\alpha_p$ . If the pumping wavelength  $\lambda_p = 1.55 \mu\text{m}$ , the effective length  $L_{\text{eff}} = 20 \text{ km}$  ( $\alpha_p \approx 0.2 \text{ dB}$ ), and, for a typical value  $A_{\text{eff}} = 50 \mu\text{m}^2$ , the Raman threshold is emerged at  $P_{0p}^{\text{th}} \approx 600 \text{ mW}$ . In the visible spectral range, a typical value  $A_{\text{eff}} = 15 \mu\text{m}^2$ , so that the threshold power  $P_{0p}^{\text{th}} \approx 10 \text{ W}$  for a 10-m fiber, which can be easily obtained making use of a YAG:Nd<sup>3+</sup> laser.

One can see that relation (8) evaluates the Raman gain of a broadband Stokes noise; therefore, it is natural that it turns out invalid for estimating the gain threshold at RS. The obtained pumping power considerably exceeds both the magnitudes usually used for the effective signal amplification in FRAs and the lasing threshold in FRLs. Really, if the pumping power equals 120–130 mW (i.e. at  $P_p \leq P_{0p}^{\text{th}}/5$ ), the Raman

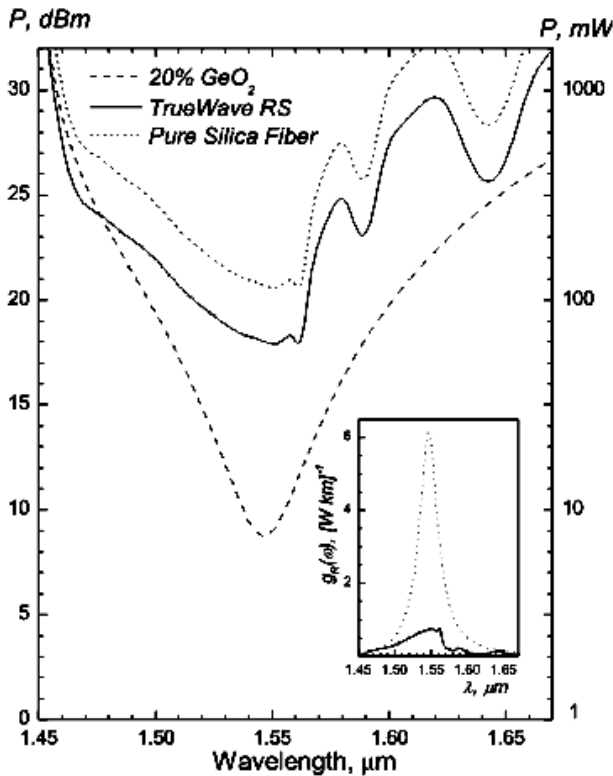


Fig. 3. Hyper-Raman emission thresholds ( $\lambda_p = 1.45 \mu\text{m}$ ) for several widely used fibers: a pure fused silica-based fiber (dotted), a TrueWave RS<sup>TM</sup> fiber (solid), and a Raman fiber with an enhanced content of GeO<sub>2</sub> (dashed curve). The Raman gain profile  $g_R(\lambda)$  of the Raman fiber in the Lorentzian approximation and a real profile for a TrueWave RS<sup>TM</sup> fiber are compared in the inset

gain is quite enough to compensate losses in a 50-km fiber [7]. In practice, the Raman laser generation can be obtained if the pumping power is several tens of milliwatts; and, if  $P_p > 1 \text{ W}$ , the efficiency of the pumping power transformation into the power of Raman lasing attains 90% [1]. Therefore, the issue concerning the minimal threshold power of Raman amplification is of practical interest and deserves a more detailed analysis. We can make necessary estimations for coupled waves directly, making use of Eqs. (4) and (5).

### 3. Simulation Results and Discussion

The conventional equations (4) and (5), which describe coupled waves during RS, make it possible to determine the hyper-Raman emission and lasing thresholds and to make quantitative estimations of their frequency dependence, basing only on the fundamental parameters of fiber's material, namely,  $g_R(\omega)$  and  $\alpha(\omega)$ .

Really, it follows immediately from Eq. (4) that, depending on the pumping power,  $dI_s/dz$  can change its sign. If there is no pumping or its power is low, we obtain  $dI_s/dz < 0$ , which corresponds to the attenuation of the Stokes wave in the course of its propagation, owing to the intrinsic losses in the fiber. A growth of the pumping intensity  $I_p$  brings about the Raman gain of the Stokes wave, which is described by the product  $g_R I_p$  and whose magnitude can exceed the intrinsic losses. In this case, the fiber becomes a gain medium, because  $dI_s/dz > 0$ , which corresponds to the increase of the Stokes wave as it propagates in the fiber. In particular, in the case  $dI_s/dz = 0$ , the fiber goes into the absolute transparency regime for a Stokes wave, in which the intensity remains constant while propagating along the fiber.

The condition of absolute fiber transparency, by its physical content, determines the lasing threshold for the SRS process. The relation  $dI_s/dz \geq 0$ , together with Eq. (4), brings about a threshold relation which looks like  $P_p(\omega) \geq \alpha_s A_{\text{eff}}/g_R(\omega)$  and, in its turn, allows one to write down the condition for hyper-Raman emission threshold at the Stokes-wave frequency  $\omega$ :

$$P_p^{\text{th}}(\omega) = \frac{\alpha_s A_{\text{eff}}}{g_R(\omega)}. \tag{9}$$

Relation (9) quantitatively describes the condition for a medium to be converted from a natural state characterized by the attenuation of a Stokes wave to a state, in which the Raman-shifted wave becomes amplified owing to the pumping. Since the function  $g_R(\omega)$  is measured experimentally and can be, therefore, considered as a known one, it is possible in a straightforward manner to calculate the threshold power of the pumping source, which allows to amplify a monochromatic Stokes wave with arbitrary frequency in the Raman spectrum range. The hyper-Raman emission threshold (9), unlike the experimental threshold (8), is governed by the parameters of a fiber medium only and does not depend on the conditions of observation, in particular, on the fiber length.

Thus, knowing the experimental data concerning the measurements of the Raman gain coefficient profile  $g(\omega)$  and the attenuation  $\alpha$  in a fiber, one can immediately determine the dependence of the hyper-Raman emission threshold at the Stokes shift frequency (or wavelength) at an arbitrary wavelength of the pumping source. Figure 3 depicts the dependences of the hyper-Raman emission threshold on the pumping wavelength in the Stokes range, if a source with  $\lambda_p = 1.45 \mu\text{m}$  is used for pumping some widely used fibers. The experimental profiles  $g(\omega)$  and the peak values of the Raman

gain coefficients  $g_{\max}$  were taken from work [10]; in particular,  $g_{\max} = 6.1 \text{ W}^{-1}\text{km}^{-1}$  for a specialized Raman fiber,  $g_{\max} = 0.4 \text{ W}^{-1}\text{km}^{-1}$  for a standard fused silica-based fiber, and  $g_{\max} = 0.74 \text{ W}^{-1}\text{km}^{-1}$  for a backbone fiber with minimized dispersion, which now dominates while creating ultra-high-speed fiber-optic transmission lines and has a TrueWave RS trademark.

For a Raman fiber, the profile  $g(\omega)$  is described satisfactorily in the framework of the simplified Lorentzian approximation [11], whereas, in the case of other fibers, it is necessary to use a more complicated but exact model of the multimode decomposition of a Raman spectrum [5]. The inset in Fig. 3 exhibits the calculation profiles of the Raman gain  $g(\omega)$  for a Raman fiber (dotted curve) and a TrueWave RS<sup>TM</sup> one. For convenience, the absolute values of optical power are expressed in terms of dBm (decibels per 1 mW – on the left ordinate axis) and mW (on the right one) units. Figure 3 demonstrates that the gain mode for a monochromatic Stokes signal with  $\lambda_s = 1.55 \mu\text{m}$  becomes switched on at the following pumping powers  $P_p$  ( $\lambda_p = 1.45 \mu\text{m}$ ): 8.9 dBm (7.8 mW) for a specialized Raman fiber, 18.0 dBm (63 mW) for a TrueWave RS<sup>TM</sup> fiber, and 20.7 dBm (117.5 mW) for a standard fused silica-based fiber.

While calculating the hyper-Raman emission threshold (see Fig. 3), the intrinsic losses at the Stokes frequency were taken equal to  $\alpha = 0.2 \text{ dB/km}$ , at which the Raman fiber can become an active laser medium if the pumping power is lower than 10 mW.

It should be noted that a substantial gain enhancement for the Raman fiber can be achieved in the course of its fabrication owing to the increased content of  $\text{GeO}_2$  (typically, of about 20%); however, this process is unfortunately accompanied by a substantial growth of intrinsic losses in the fiber with minimal values  $\alpha \approx 0.3 \div 1.0 \text{ dB/km}$ . Therefore, in Fig. 4, we present the dependences of the hyper-Raman emission threshold ( $\lambda_p = 1.45 \mu\text{m}$ ) for various Raman fibers with different values of intrinsic losses ranging from 0.2 to 1.0 dB/km. If the intrinsic losses increase within this interval, the threshold power for a monochromatic Stokes signal at  $\lambda_s = 1.55 \mu\text{m}$  increases in a natural manner from about 9 to 40 mW. At subthreshold values of the pumping power, which correspond to the shadowed region in Fig. 4, the Stokes waves become attenuated; the Raman amplification is realized in the light region above the curves.

The results of calculations testify that if the pumping power reaches several hundred milliwatts, the lasing threshold for a monochromatic Stokes signal takes place

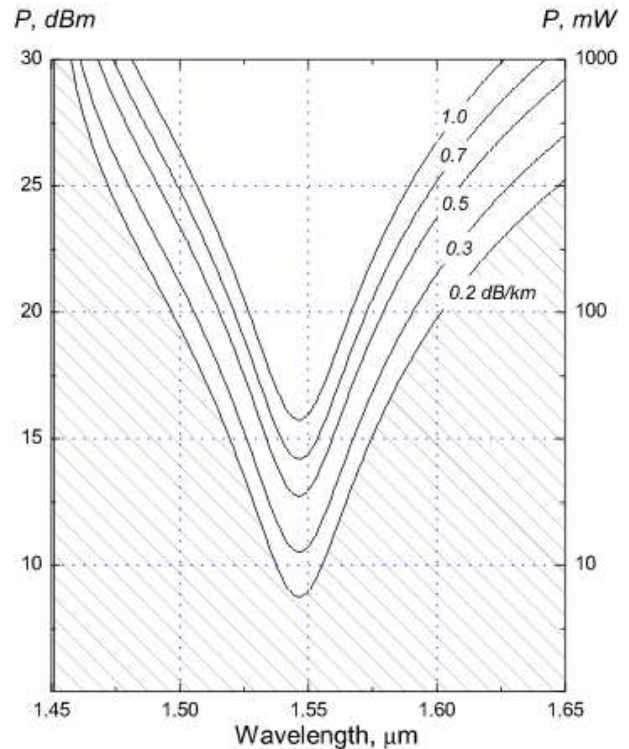


Fig. 4. Raman lasing threshold ( $\lambda_p = 1.45 \mu\text{m}$ ) as a function of the wavelength for Raman fibers with various intrinsic losses. The Stokes wave becomes attenuated in the shadowed region; Raman amplification is realized in the light region above curves

in a rather wide spectral range irrespective of actual losses in the fiber. In this case, for the pumping with  $\lambda_p = 1.45 \mu\text{m}$ , the optical signal gain and laser generation can be obtained in the range from 1.5 to 1.6  $\mu\text{m}$ , i.e. in the whole interval of maximal fiber transparency. We should emphasize once more that the spectral position of the lasing band can be shifted by a simple variation of the pumping wavelength. In so doing, the absolute values of threshold power can be found if one makes allowance for the frequency dependences of the fiber parameters, namely, the Raman gain coefficient  $g(\omega)$  and the attenuation  $\alpha(\omega)$ .

The quoted results are confirmed by numerous experimental data obtained recently. For instance, the intensive Raman lasing at three laser wavelengths of 1236, 1316, and 1407 nm was observed, when the pumping power of a  $\text{Nd}^{3+}$ -laser ( $\lambda_p = 1062 \text{ nm}$ ) did not exceed 200 ÷ 300 mW. In work [9], a report was made about a six-wavelength Raman laser with controlled output power of 0–330 mW, which had a single Yb fiber source of pumping with  $\lambda_p = 1100 \text{ nm}$  and  $P_p \approx 1.3 \text{ W}$ . The direct extrapolation of those and other experimental

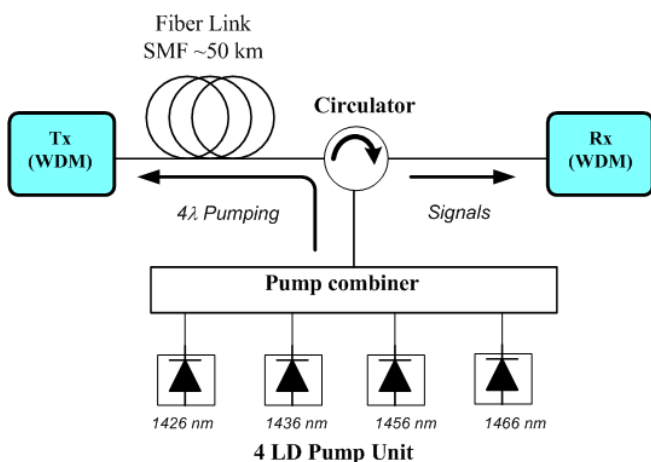


Fig. 5. Scheme of Raman amplification using a 4-LD pumping source

data to the threshold power of hyper-Raman emission testifies that, depending on the type of a Raman silica fiber, the threshold value falls within the interval  $5 \div 100$  mW. This agrees with our calculations and proves the validity of the suggested model.

Hence, relation (9) gives a quantitative estimation for the minimal level of a pumping power  $P_p$ , which ensures the laser gain threshold for a monochromatic Stokes wave with arbitrary frequency  $\omega$ . The practical realization of specific devices is accompanied, as usual, by extra expenses of pumping power which are necessary for the compensation of losses in external elements of the optical scheme. Therefore, the value of  $P_p$  obtained from Eq. (9) corresponds to a theoretical minimum of pumping power needed for the lasing threshold to be reached, which defines the purpose for the optimization of FRL parameters.

The suggested approach is useful enough to analyze the gain dynamics of a monochromatic wave in a distributed FRA. Equation (9), which determines the mode of absolute fiber transparency, enables one to make the direct estimations of the gain properties at any given point of the fiber and at any frequency  $\omega$  of the Stokes wave, if the magnitude of pumping power at this point is known. Moreover, the analysis can be directly generalized onto the case of an arbitrary number of optical signals and pumps. In this case, the mode of absolute fiber transparency for the  $i$ -th monochromatic Stokes wave is associated with a singular point in the corresponding reduced equation.

In the last section, we illustrate how the results of numerical calculations made for the FRL threshold can be applied to the analysis of a particular realization of the multiwavelength pumping source for an FRA.

#### 4. Application

In order to extend the range of operation frequencies, we have analyzed a specific example of the practical realization of FRA. We proposed an FRL-based scheme for the modernization of the latter, in which the results of calculations of the lasing threshold were taken into account. Preliminarily, we have studied a commercial specimen of the FRA, which had four laser diodes (LDs) – as a pumping source – with emission wavelengths of 1426, 1436, 1456, and 1466 nm. The amplification of optical signals was observed in a single-mode fiber in the counter direction to the pumping (see the scheme in Fig. 5). The maximal pumping power was 300 mW for each LD. A pump combiner was used to direct the output emission generated by each LD through a circulator into a fragment of a standard 50-km single-mode fiber. The pump source allowed the power of each LD to be set independently within the range from 0 to 300 mW using a digitized control block. At the receiving end of the line, the output optical signals from the fiber, after their transmission through a circulator, were registered by an optical spectrum analyzer.

As a result of the test control together with a spectroscopic simulation of the device [11], it was found that the working bank of the FRA entirely covers the C-band telecommunication window which is conventionally allocated for optical signal transmission. The calculated bandwidth of the FRA at a 1-dB level was 50 nm in the range from 1520 to 1570 nm, with the gain ripple being no more than 0.5 dB; those parameters completely corresponded to the values of 1528–1562 nm that had been indicated in the manufacturer's specifications. Simultaneously, it turned out that such a 4λ amplifier had a drop of the gain coefficient in the L-band which exceeded 10 dB and could not be overcome by pumping; this circumstance made it inapplicable for the signal amplification in the long-wavelength telecommunication window. However, it is known [12] that, for a functioning distributed Raman amplifier, the interaction between short- and long-wavelength pumping sources in the course of signal propagation in a fiber usually gives rise to a significant increase of the pumping power for long-wavelength sources. For equalizing the gain coefficient of the FRA that operates according to the scheme with several pumping sources, it is necessary to lower the input power of long-wavelength pumpings. Therefore, in a real device, only about 10% of the nominal power of long-wavelength pumpings are used, as a rule, for amplification.

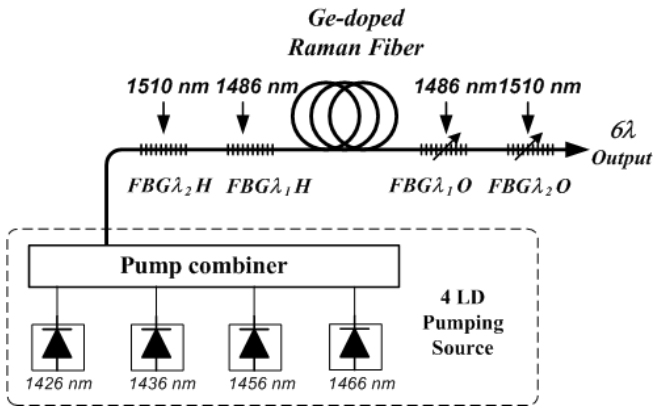


Fig. 6. Scheme of a modified  $6\lambda$  pumping source for an FRA with an extended bandwidth that covers the combined C+L-band

The resulting excess of the pumping power can be used to generate additional pumpings with different wavelengths, making use of FRLs with Bragg grating cavities. The simulation testifies that the available gain bandwidth of FRA can be extended onto the whole L-band, provided that only two additional sources of pumping with wavelengths of 1486 and 1510 nm are used. The scheme of a multiwavelength pumping source, which generates the six-wavelength laser lasing and enables the gain bandwidth of FRA to be extended over the whole L-band, is demonstrated in Fig. 6. The source includes 4 pumping LD (with  $\lambda_p = 1426, 1436, 1456,$  and  $1466$  nm) directly coupled in a rather short fragment of a Raman fiber with two grating cavities (for wavelengths of 1486 and 1510 nm), which are located at the fiber ends. As a result, we obtain a  $6\lambda$  pumping source which allows the operational bandwidth of the FRA to be so extended that it would cover the combined C+L-band with a satisfactory level of gain ripple.

The calculated frequency characteristics of FRA with  $4\lambda$  or  $6\lambda$  pumping are compared in Fig. 7. The  $6\lambda$  pumping amplifier demonstrates a wide amplification bandwidth, over 80 nm, with a low gain ripple that does not exceed 0.5 dB. The minimization of the gain ripple was achieved by adjusting the output power of each pumping source. The minimal gain ripple ( $< 0.5$  dB) within the total combined C+L-band can be obtained under the condition that the effective pumping powers

**Pumping power thresholds for Raman lasers with the wavelength  $\lambda_l$  and pumping at  $\lambda_p$**

$\lambda_p, \text{ mW}$	$\lambda_l = 1.486, \text{ mW}$	$\lambda_l = 1.510, \text{ mW}$
1.426	42.6	9.7
1.436	69.6	20.3
1.456	144.0	62.7
1.466	190.9	93.9

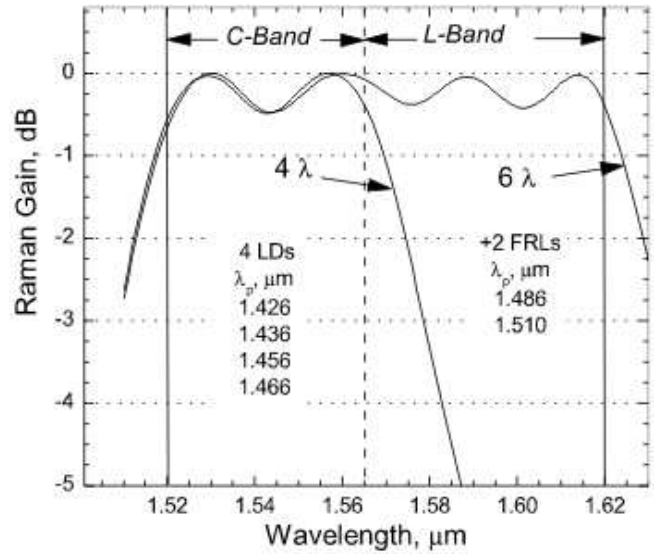


Fig. 7. Comparison between the frequency characteristics of FRAs with  $4\lambda$  and  $6\lambda$  pumping sources

relate to each other as  $0.8 : 1.0 : 0.75 : 0.7 : 1.1 : 1.5$ , if counting from the minimal to the maximal wavelength of individual sources.

In Fig. 8, the dependences of the threshold power on the wavelength are depicted for each pumping source, provided 0.2-dB/km fiber losses (panel a). Panel b exhibits the same dependences but for a 1426-nm source and various fiber losses. The numerical values of the power, which is consumed by each LD source and ensures the Raman lasing threshold in two additional Raman pumping lasers with Bragg grating-base cavities, are quoted in Table. One can see that pumping both FRLs at 1486 and 1510 nm is quite feasible for any of the available LD sources.

### 5. Conclusions

To summarize, the conditions for the lasing threshold to emerge, provided the stimulated Raman interaction between monochromatic waves – pumping and Stokes emission ones, – have been studied. The conditions are examined in a general theoretical sense as those that ensure the absolute transparency regime of the fiber. This mode arises under the influence of the pumping which converts the fiber core into the state of gain medium for a monochromatic optical wave. Adopting such a definition, the lasing threshold is expressed only in terms of material parameters of the fiber and does not depend on the observation conditions, in particular, on

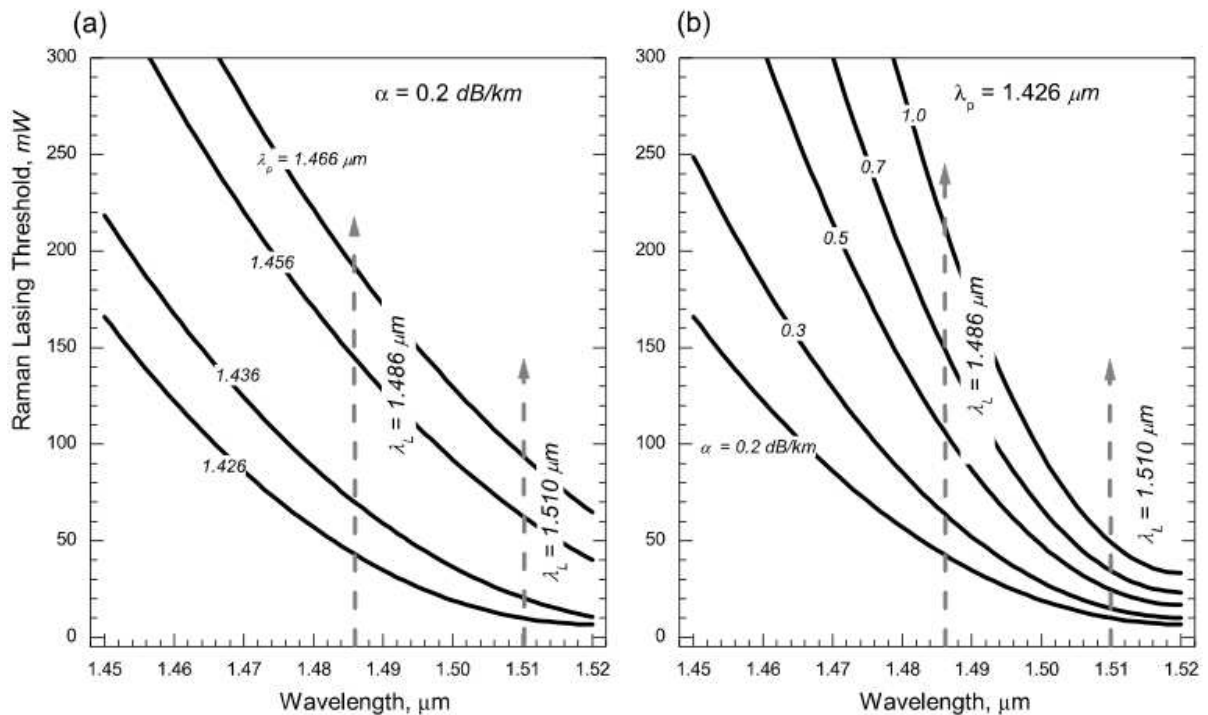


Fig. 8. Frequency dependences of the pumping power threshold, which ensures the Raman lasing threshold for various pumping wavelengths (a) and various values of the intrinsic losses in a Ge-doped fiber (b). For a Raman fiber with  $\text{GeO}_2$ ,  $g_{\max} = 6.1 \text{ W}^{-1}\text{km}^{-1}$  [10]. The spectral position of FRL lines at 1486 and 1510 nm are marked by dashed arrows

the fiber length. Directly from the standard equations for coupled waves which describe the interaction between a pumping wave and the Stokes emission, a simple analytical expression for the determination of the hyper-Raman emission threshold has been derived. The relation obtained has been applied to calculate the lasing threshold for a monochromatic Stokes wave with arbitrary frequency in some single-mode fibers.

The dependences of the hyper-Raman emission threshold on the frequency have been plotted for a number of widely used fibers. A possibility of the quantitative calculation of the lasing threshold for an arbitrary frequency from the Stokes-shift range has been demonstrated, and the numerical values for the pumping power threshold have been presented. Since the threshold values correspond to a theoretical minimum for the pumping power which makes the Raman lasing possible, they can be used in practice as a criterion of the parameter optimization for Raman fiber-optic lasers. The suggested approach turns out also useful when analyzing the dynamics of the amplification of monochromatic waves in distributed Raman amplifiers. The results of numerical calculations

have been applied to determine the threshold of Raman lasers which are included into the pumping block of an experimental Raman amplifier and are connected in a multiwavelength pumping circuit design. Note that the given analysis admits a straightforward generalization onto the case where there are a number of optical signals and several pumping wavelengths; so that it can be applied for the further development of real Raman amplifiers.

1. E.M. Dianov and A.M. Prokhorov, IEEE J. Select. Topics Quant. Electron. **6**, 1022 (2000).
2. M.N. Islam, IEEE J. Select. Topics Quant. Electron. **8**, 548 (2002).
3. R.H. Stolen, E.P. Ippen, and A.R. Tynes, Appl. Phys. Lett. **20**, 62 (1972).
4. G.P. Agrawal, *Nonlinear Fiber Optics*, 2nd ed. (Academic, San Diego, Ca, 1995).
5. G.S. Felinskyi, in *Proceedings of the 7th International Conference on Laser and Fiber-Optical Networks Modeling (LFNM 2005)*, Yalta, Ukraine, September 12–17, 2005 (NURE Kharkiv, IEEE CN 05TH8810, 2005) p. 262.
6. J. Bromage, K. Rottwitt, and M.E. Lines, IEEE Photon. Technol. Lett. **14**, 24 (2002).
7. R.H. Stolen, C. Lee, and R.K. Jain, J. Opt. Soc. Am. B **1**, 652 (1984).

8. R.H. Stolen, J.P. Gordon, W.J. Tomlinson, and H.A. Haus, *J. Opt. Soc. Am. B* **6**, 1159 (1989).
9. H. Kidorf, K. Rottwitt, M. Nissov, M. Ma, and E. Rabarjaona, *IEEE Photon. Technol. Lett.* **11**, 530 (1999).
10. K. Rottwitt, J. Bromage, A.J. Stentz, L. Leng, M.E. Lines, and H. Smith, *J. Lightwave Techn.* **21**, 1652 (2003).
11. G.S. Felinskyi and P.A. Korotkov, in *Proceedings of the 2nd International Conference on Advanced Optoelectronics and Lasers (CAOL 2005), Yalta, Ukraine, September 12–17, 2005* (NURE Kharkiv, IEEE CN 05TH8809, 2005) Vol. 2, p. 168.
12. M.D. Mermelstein, C. Horn, S. Radic, and C. Headley, *Electronics Lett.* **38**, 636 (2002).

Received 05.09.06.

Translated from Ukrainian by O.I. Voitenko

#### ОСОБЛИВОСТІ ВИНИКНЕННЯ ВКР-ПІДСИЛЕННЯ МОНОХРОМАТИЧНОГО СВІТЛА В КВАРЦОВИХ ОДНОМОДОВИХ ВОЛОКНАХ

*П.А. Коротков, Г.С. Фелінський*

#### Р е з ю м е

Вимушене комбінаційне розсіяння (ВКР) світла є основою роботи таких пристроїв фотоніки, як волоконно-оптичні лазери та волоконно-оптичні підсилювачі. На відміну від феноменологічного визначення порога ВКР у ранніх експериментах у цій роботі проведено аналіз порога ВКР супервипромінювання в одномодових волокнах з точки зору строгого описання підсилення в активних лазерних матеріалах. Показано, що порогову умову ВКР для монохромної оптичної хвилі сигналу можна отримати безпосередньо зі стандартних рівнянь для зв'язаних хвиль з використанням тільки фундаментальних параметрів волокна. Наведено кількісні залежності лазерного порога від довжини хвилі у деяких широко застосовуваних волокнах.